A cold ^{87}Rb atomic beam*

Wang Xiao-Jia(王晓佳)[a)b)], Feng Yan-Ying(冯焱颖)[b)c)†], Xue Hong-Bo(薛洪波)[b)], Zhou Zhao-Ying(周兆英)[b)], and Zhang Wen-Dong(张文栋)[a)]

[a)] *Key Laboratory of Instrumentation Science and Dynamic Measurement, Ministry of Education, North University of China, Taiyuan* 030051, *China*

[b)] *State Key Laboratory of Precision Measurement Technology and Instruments, Department of Precision Instruments and Mechanology, Tsinghua University, Beijing* 100084, *China*

[c)] *Joint Institute of Measurement Science (JMI), National Institute of Metrologia–Tsinghua University, Beijing* 100084, *China*

(Received 29 June 2011; revised manuscript received 24 September 2011)

We demonstrate an experimental setup for the production of a beam source of cold ^{87}Rb atoms. The atoms are extracted from a trapped cold atomic cloud in an unbalanced three-dimensional magneto–optical trap. Via a radiation pressure difference generated by a specially designed leak tunnel along one trapping laser beam, the atoms are pushed out continuously with low velocities and a high flux. The most-probable velocity in the beam is varied from 9 m/s to 19 m/s by varying the detuning of the trapping laser beams in the magneto–optical trap and the flux can be tuned up to 4×10^9 s^{-1} by increasing the intensity of the trapping beams. We also present a simple model for describing the dependence of the beam performance on the magneto–optical trap trapping laser intensity and the detuning.

Keywords: continuous atomic beam, unbalanced three-dimensional magneto–optical trap, radiation pressure difference, laser cooling and trapping

PACS: 67.85.–d **DOI:** 10.1088/1674-1056/20/12/126701

1. Introduction

Low-velocity intense atomic beam sources are of increasing significance in a variety of atom optics experiments and applications, such as new atomic clocks,[1] novel precision experiments,[2] atom interferometry[3] and lithography.[4] The exploration of the vast area of new physics is made accessible by the routine production of the Bose–Einstein condensates.[5] In particular, they are especially important in the development of space-qualified experiments, because microgravity conditions in space do not support the use of atomic fountains.[6] A continuous high flux atomic source that is comparable to the pulsed atomic beams or the atomic fountain using pulsed sources helps to achieve a good signal-to-noise ratio and enhances the ultimately achievable phase resolution of the interferometer, which is given by the atomic shot-noise limit.[7]

There are two different methods and techniques to generate the low-velocity intense atomic beams, one is by directly laser decelerating thermal atomic beams, the other is by laser accelerating an ensemble of atoms from the laser cooled atomic trap. The former method can be achieved by using the Zeeman-slowing technique,[8,9] chirped lasers,[10] etc. It usually requires a spatial distance to cool the atomic beams to the expected velocities and has been accompanied by a serious loss of atomic flux.[11] The latter method can be achieved by extracting slow atomic beams from an atomic trap, which can be the vapor-cell magneto–optical trap (MOT) or the pyramidal MOT,[12−15] and hence it can greatly improve the system compactness. Lu *et al.* developed a low velocity intense source (LVIS) of atoms by using a specially fabricated mirror with a 1-mm hole at the centre of the MOT, and the source reached a flux of 5×10^9 atoms/s.[16]

In this paper, we propose an improved design of Lu's,[17] which produces a rubidium atomic beam with a parabolic trajectory to eliminate the effect of the pushing laser on atoms after they leave the beam source. The stray light from the pushing laser is an important noise source and a limiting factor for improving the sensitivity of beam-based spectroscopic mea-

*Project supported by the National Natural Science Foundation of China (Grant No. 50775127), the Major State Basic Research Development Program of China (Grant No. 2010CB922901), and the Independent Research Projects of Tsinghua University, China (Grant No. 2009THZ06).

†Corresponding author. E-mail: yyfeng@mail.tsinghua.edu.cn

© 2011 Chinese Physical Society and IOP Publishing Ltd

surements, such as atomic frequency standards and atomic interferometers.

2. Experimental setup

As shown in Fig. 1, the whole experimental setup is based on a two-chamber vacuum system that consists of a three-dimensional (3D) MOT system and a probing system for the atomic beam. The two chambers are connected only by a 1-mm hole. In the MOT chamber, the unbalanced 3D MOT is produced and the atomic beam is generated from the trapped cold atomic cloud. In the probing chamber, the atomic beam is measured through the fluorescence and the time of flight (TOF) technologies. With the help of two ion pumps (Varian USD 8500), the two chambers operate under background pressures of 8×10^{-10} Torr (1 Torr=1.33322×10^{2} Pa) and 2×10^{-9} Torr respectively when the rubidium reservoir, which is connected to the MOT chamber through a valve, is turned off. When the rubidium reservoir is turned on and heated to about 36 °C–40 °C, the rubidium vapour enters into the MOT chamber, and the chamber pressure increases rapidly to $\sim 10^{-7}$ Torr, while it has little effect on the probing chamber pressure. The windows of the vacuum chamber are coated with broadband near-IR antireflection coatings, and they are attached to the chamber using indium wire for sealing. Inside the chamber, an ensemble of retro-reflecting optics, consisting of a 0° mirror with a $\lambda/4$ plate on top of it, is installed. Both elements are of 50.8 mm in diameter, and each has a 1-mm hole in the centre. A pipe of copper foam is placed just after the hole for absorbing residual atoms leaking out of the MOT chamber into the probing chamber. In order to avoid the laser–atom interaction, the cold ^{87}Rb atomic beam is injected into the probing chamber at a small angle. The light (the straight line in Fig. 1) goes in a straight line, and the atomic beam (the curved line in Fig. 1) will be separated from the pushing light with the help of gravity.

A quadrupole magnetic field for the MOT is generated using a pair of anti-Helmholtz coils, which are oriented along the atomic beam axis outside the MOT vacuum. The requirement is to have both the field and the field gradient to be zero along the symmetry axis of the chamber. A current of 1.2 A–1.5 A per coil produces a transverse field gradient of 10 Gs/cm–15 Gs/cm (1 Gs=10^{-4} T). Three pairs of Helmholtz coils provide an orthogonal bias magnetic field to compensate the earth's magnetic field and other stray fields from the nearby ion pump, etc. and are used to adjust the trapping position for optimizing the number of trapped atoms, aligning it with the beam ejection hole, and therefore optimizing the atomic beam flux.

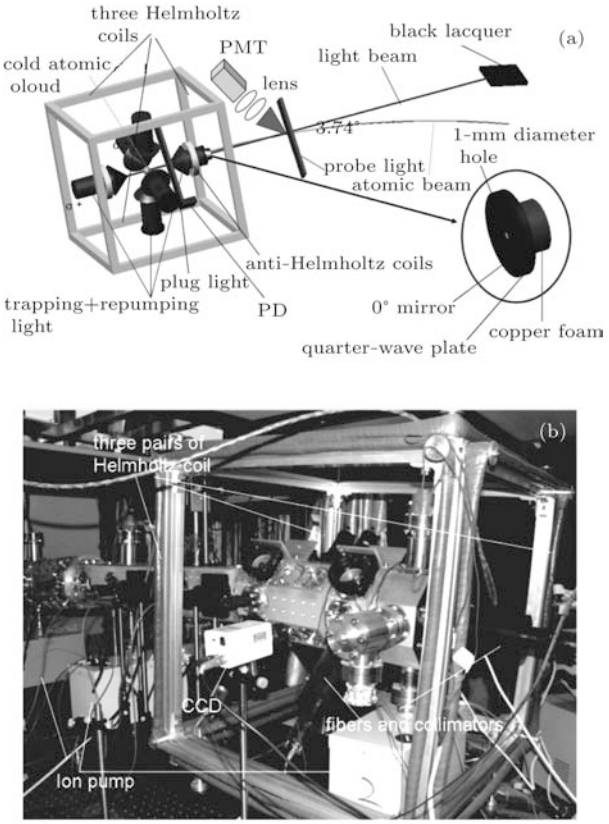


Fig. 1. (a) Schematic diagram of the experimental setup and the optical probe configuration for characterizing the atomic beam. PMT stands for photomultiplier tube. (b) Photo of realized MOT and probing chambers, the fibre system, and the collimator.

The light beams for the operation and the probing of the cold atom source are generated by a laser system. Two external-cavity diode lasers (Toptica DLX110 and Toptica DL100) and an amplifier (Toptica TA) are used for the trapping and repumping beams, and a single diode laser (Toptica DLpro) produces the probing beam. All lasers are locked via grating feedback from the saturated absorption spectroscopy. The DLX110 diode locked to the cross-over line between the $5s^2S_{1/2}(F=2)\rightarrow5p^2P_{3/2}(F'=2)$ and $5s^2S_{1/2}(F=2)\rightarrow5p^2P_{3/2}(F'=3)$ transition provides the trapping light at a typical 30 MHz detuned from the $5s^2S_{1/2}(F=2)\rightarrow5p^2P_{3/2}(F'=3)$ transition after an additional 110-M (1 M=1 mol/dm^3) AOM frequency shifting. The frequency of the repumping beams is locked on the $5s^2S_{1/2}(F=2)\rightarrow5p^2P_{3/2}(F'=2)$ transition. Finally, the trapping light and the re-

pumping light are coupled using a beam splitter (BS) and a fibre coupling, injected into the amplifier, split into three parts by a fibre splitter, and led to the MOT chamber.

A fibre system is used to transfer the light from the optical table to the vacuum apparatus. All the fibres are polarization maintaining and connected to the collimators, which are fixed on the chambers. Each collimator consists of a $\lambda/2$ plate, a polarized beam splitter (PBS), a $\lambda/4$ plate, and a collimation lens with a focal length of 200 mm. We can get three collimated Φ44 mm σ^+ or σ^- beams with adjustable intensities via the collimators. These beams are reflected back in the opposite directions by three ensembles of retro-reflecting optics, including the optics with the hole in the vacuum, which makes six counter propagating laser beams in the MOT chamber. Then we get the unbalanced 3D MOT with an atomic beam in it. Figure 2 is a CCD camera image of a formed atom beam, which is taken through a window in the MOT vacuum and allows us to verify the existence of the atomic beam.

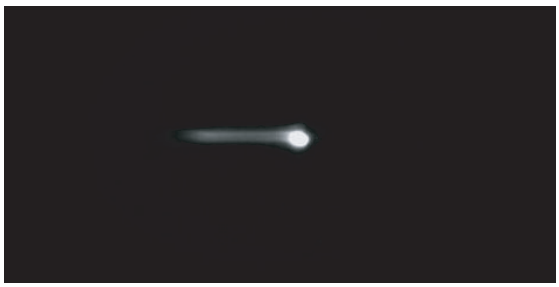


Fig. 2. A fluorescence picture of atomic cloud and beam in the 3D MOT.

3. Modeling

A numerical analysis is done to model the atomic beam characteristics. The Rb atoms are trapped in the MOT and pushed through the 1-mm hole by the spontaneous force from the so-called acceleration beam, one of the six trapping laser beams. This force on the atoms is given by[18]

$$F_{\rm sp} = \frac{\hbar k S_0 \gamma/2}{1 + S_0 + (2\delta/\gamma)^2}, \tag{1}$$

where S_0 is the saturation factor for the laser beam, $\hbar k$ is the photon momentum, γ is the natural linewidth of the atomic transition, and δ is the off-resonance detuning of the acceleration laser. The acceleration laser beam interacts with the Rb atoms in the $m_{\rm F} = +1$ level in the acceleration region. In the vicinity of the MOT, the Zeeman shift $\Delta\delta_{\rm B}$ increases approximately linearly as the Rb atoms move out of the MOT. As the Rb atoms gain their speed, the Doppler shift $\Delta v_{\rm D}$ also adds to the effective off-resonance detuning. We therefore obtain the total off-resonance detuning for Eq. (1) as

$$\delta_{\rm total} = \delta_0 + \Delta\delta_{\rm B} + \Delta v_{\rm D}, \tag{2}$$

where δ_0 is the fixed detuning of the acceleration laser. Substituting Eq. (2) into Eq. (1), we obtain

$$F_{\rm sp} = \frac{\hbar k S_0 \gamma/2}{1 + S_0 + [2(\delta_0 + \Delta\delta_{\rm B} + \Delta v_{\rm D})/\gamma]^2}. \tag{3}$$

In a similar way, we can also obtain the effect of the optical repumping laser from Eq. (1). The off-resonance detuning is the Zeeman shift $\Delta\delta_{\rm Br}$ and the Doppler shift. The Doppler effects can be ignored as the repumping laser beam propagates perpendicularly to the atomic beam. This effect is incorporated into the model, and we obtain

$$\begin{aligned} F_{\rm sp} = & \frac{\hbar k S_0 \gamma/2}{1 + S_0 + [2(\delta_0 + \Delta\delta_{\rm B} + \Delta v_{\rm D})/\gamma]^2} \\ & \times \frac{{\rm a}\hbar k S_{0{\rm r}} \gamma/2}{1 + S_{0{\rm r}} + [2\Delta\delta_{\rm Bb}/\gamma]^2}, \end{aligned} \tag{4}$$

where $S_{0{\rm r}}$ is the saturation factor for the optical repumping laser beam, and a is a proportional constant. Ignoring the initial thermal velocity of the cold atoms in the beam, we obtain the acceleration of the Rb atom and therefore the velocity of the beam. The acceleration is given by

$$\begin{aligned} a_{\rm atom} = & \frac{F_{\rm sp}}{m_{\rm Rb}} = \frac{\hbar k S_0 \gamma/2 m_{\rm Rb}}{1 + S_0 + [2(\delta_0 + \Delta\delta_{\rm B} + \Delta v_{\rm D})/\gamma]^2} \\ & \times \frac{{\rm a}\hbar k S_{0{\rm r}} \gamma/2 m_{\rm Rb}}{1 + S_0 + [2\Delta\delta_{\rm Br}/\gamma]^2}, \end{aligned} \tag{5}$$

where t_l is the time of the atoms flying out of the trapping and repumping region, in which the Rb atom absorbs photons and is accelerated.

The atom flux of the source is proportional to the loading rate of the MOT,[19] which is given by

$$R_{\rm MOT} = \frac{n_{\rm b} V^{2/3} v_{\rm cap}^4}{2\alpha^3} = \frac{1}{2} n_{\rm b} S v_{\rm cap}^4 \left(\frac{m}{2k_{\rm B}T}\right)^{3/2}, \tag{6}$$

where V and S are the volume and the surface area of the MOT cell, respectively, $n_{\rm b}$ is the background density, $\alpha = (2k_{\rm B}T/m)^{1/2}$ is the most probable velocity of the atoms in the MOT, and $v_{\rm cap}$ is the capture velocity given by

$$v_{\rm cap} \approx \gamma\lambda/\pi. \tag{7}$$

The capture velocity mainly depends on the physical properties of the Rb atom. The flux of the atom with time can be expressed by

$$\Phi_{\rm flux} = \frac{{\rm d}N}{{\rm d}t} = R_{\rm MOT} - N/\tau, \tag{8}$$

where τ is the average time between two collisions with the background atoms.

The flux is also limited by the MOT parameters, such as the intensity and detuning of the trapping laser beams. These effects can be deduced by incorporating the total scattering rate $\gamma_{\rm p}$ into Eq. (8). Then we obtain the model of the atomic beam

$$\begin{aligned}\Phi_{\rm flux} &= \frac{{\rm d}N}{{\rm d}t}\mu_{\rm p}\gamma_{\rm p} \\ &= (R_{\rm MOT} - N/\tau)\frac{\mu_{\rm p}S_0\gamma/2}{1+S_0+(2\delta_{\rm total}/\gamma)^2},\end{aligned} \tag{9}$$

where $\mu_{\rm p}$ is a proportional constant.

4. Characterization and analysis

To measure the flux of an atomic beam, a 0.5-mW/cm^2 probing beam with width 1 mm is aligned orthogonal to the atomic beam inside the probe chamber, and the laser frequency is swept across the resonance or locked on the $5{\rm s}^2{\rm S}_{1/2}(F=2)\rightarrow 5{\rm p}^2{\rm P}_{3/2}(F'=3)$ transition. The resonance fluorescence signal from the atomic beam is detected using a photomultiplier tube (PMT, Hamamatsu H7422-50) placed outside the vacuum chamber.

The fluorescence detection system allows the determination of the total flux of the atomic beam from the fluorescence signal of the beam. For a cold-atom beam traveling with mean velocity $\langle v_z\rangle$ through a resonant probe laser with diameter Δz, the integrated atom flux $\Phi_{\rm flux}$ is given by[14]

$$\begin{aligned}\Phi_{\rm flux} &= \frac{U_0}{G_{\rm PMT}R\eta(\lambda)\cdot e}\frac{4\pi}{{\rm d}\Omega}\frac{1}{K_{\rm lens}^4} \\ &\quad\times\frac{v_z}{\Delta z}\left(\frac{2}{\Gamma}\frac{1+S_{0\rm p}}{S_{0\rm p}}\right),\end{aligned} \tag{10}$$

where U_0 is the fluorescence signal collected by the PMT of the detection system with detector efficiency $\eta(\lambda)$ and collection solid angle ${\rm d}\Omega$, $S_{0\rm p} = I/I_{\rm sat}$ is the saturation parameter for the probe laser, I and $I_{\rm sat}$ are the acceleration laser intensity and the saturation intensity for the atomic transition, respectively, Γ is the natural linewidth of the atomic transition, $G_{\rm PMT}$ is the gain of the PMT, and $K_{\rm lens}$ is the transmittance of the lenses. In our PMT collection system, the collection solid angle ${\rm d}\Omega$ is 0.18 sr.

The longitudinal velocity and the velocity distribution of the atomic beam are measured using the TOF method by suddenly switching off the atomic beam. This is accomplished by switching on an additional resonant "plug" laser beam that pushes the atoms away from the axis before they reach the exit aperture, as shown in Fig. 1. In our system, a 1 mm×10 mm plug laser beam with a power of $\sim$ 20 mW is placed 10 mm away from the centre of the MOT and is turned on or off by using a mechanical shutter. The accuracy influence of the longitudinal velocity caused by the mechanical shutter is about 0.2 m/s. When making measurements, the plug beam is unblocked so that the atoms are forced out of the extraction column and returned to the centre of the trap.

From the decay of the fluorescence signal $\Phi_{\rm fl}$ as a function time (Fig. 3(a)), we obtain the apparent TOF distribution, which is proportional to ${\rm d}\Phi_{\rm fl}/{\rm d}\tau$ and can be transformed into the axial velocity distribution using the flight distance L of 220 mm. The procedure is illustrated in Fig. 3 for a push-beam intensity of $I = 6$ mW/cm^2 and a detuning of $\delta_0 = 5.5\Gamma$. We can

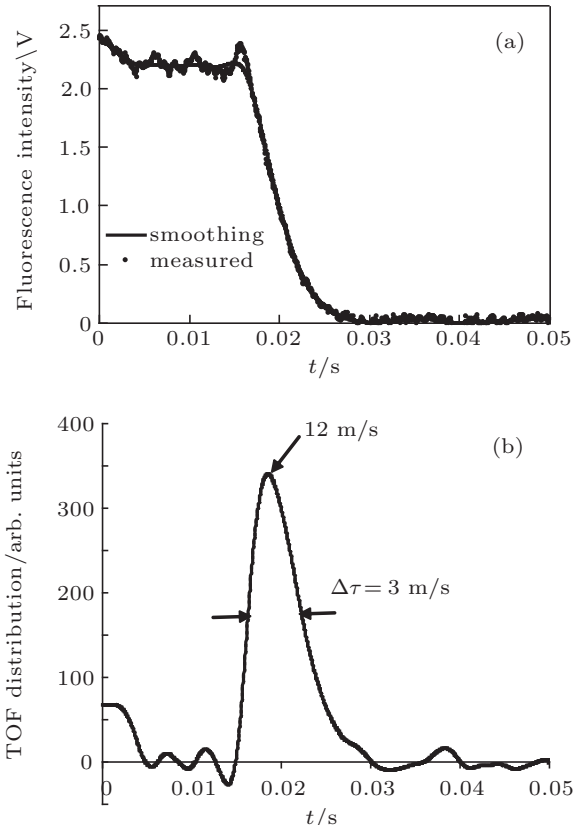


Fig. 3. (a) Fluorescence signal curve of the atomic beam using the TOF. (b) The TOF velocity distribution of the atomic beam. The smoothing solid line is the derivative of the solid line in panel (a).

get the mean apparent arrival time $\tau = 18$ ms and the full width at half maximum (FWHM) $\Delta\tau = 3$ m/s. Therefore the most-probable velocity $v_{\rm p} = 12$ m/s is given by L/τ and the flux of the atomic beam $\Phi_{\rm flux} = 4 \times 10^9$ s^{-1} is given by Eq. (10). The resulting velocity distribution of the atoms extracted from the MOT is presented in Fig. 3(b).

We obtain a maximum atomic flux of $\sim 4.5 \times 10^9$ s^{-1} by adjusting the intensity and the detuning of the trapping laser beams. Figure 4 characterizes the dependence of the atomic beam flux on MOT trapping laser detuning. The maximum values for the atomic flux are observed under trapping laser detuning of about 4.5 Γ. Figure 5 characterizes the dependence of the atomic beam flux on the MOT trapping laser intensity. As shown as Fig. 5, we can get the saturation intensity of 2.8 mW/cm^2 for the atomic beam flux. When the trapping laser intensity is lower than 2.8 mW/cm^2, the atomic beam flux reduces rapidly. And the beam flux remains essentially unchanged after the intensity reaches 2.8 mW/cm^2.

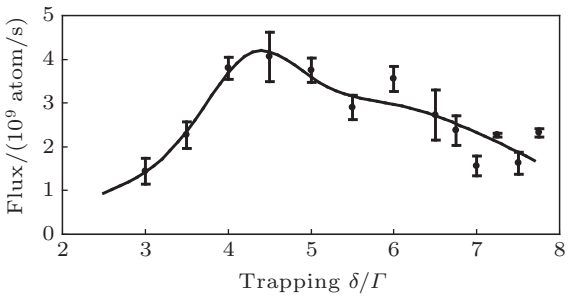


Fig. 4. Dependence of atomic-beam flux on laser detuning (with $I_{\rm trapping} = 6.7$ mW/cm^2). The points with the standard deviations are the result of the measurement. The continuous curve is the result of the fitting.

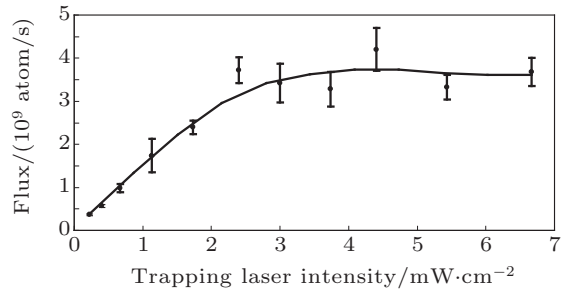


Fig. 5. Dependence of atomic-beam flux on trapping laser intensity (with $\delta_{\rm trapping} = 4.4\Gamma$). The points with standard deviations are the result of measurement. The continuous curve is the result of fitting.

We present the experimental study of the phenomenon and can explain the results with the above theoretical model of Eq. (9). By adjusting the detuning of the trapping laser δ_0 to an appropriate value, the total off-resonance detuning $\delta_{\rm total}$ reaches the minimum value, and the flux of the beam can obtain the maximum value. With the increasing trapping laser intensity, the value of $\Phi_{\rm flux}$ increases and then goes to a constant in the model.

Dependences of the longitudinal velocity in the atomic beam on the laser detuning and intensity are shown in Figs. 6 and 7, respectively. The experimental results are in quantitative agreement with the numerical simulations based on Eq. (5) (with $a = 90$).

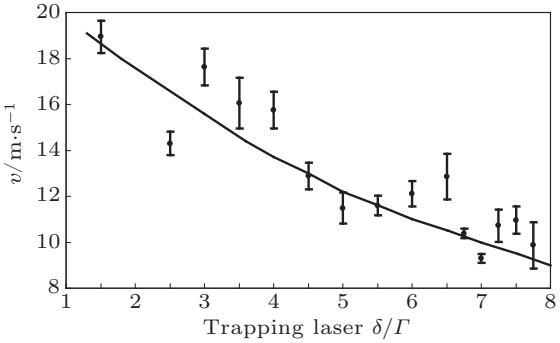


Fig. 6. Dependence of longitudinal velocity on laser detuning (with $I_{\rm trapping} = 6.7$ mW/cm^2). The continuous solid line is the numerical simulation results of the model. The points with standard deviations are experimental results.

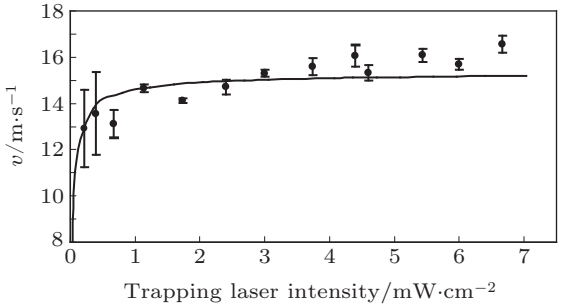


Fig. 7. Dependence of atomic-beam flux on trapping laser intensity (with $\delta_{\rm trapping} = 4.4\Gamma$). The continuous curve is the numerical simulation results of the model. The points with standard deviations are experimental results.

5. Conclusion

We have demonstrated a high-flux, low-velocity, and well-collimated atomic beam of ^{87}Rb atoms based on a 3D vapour-cell magneto–optical trap. The beam source of the ^{87}Rb atoms has been generated with a most-probable velocity of $\sim$ 12 m/s, a longitudinal FWHM velocity width of $\sim$ 3 m/s, and a tunable atomic flux from 1×10^9 s^{-1} to 4.5×10^9 s^{-1}. We present the model for describing the dependence of the beam performance on the MOT trapping laser intensity and the detuning, which is well validated by the

experimental results. Future works will be focused on improving the stability of the beam source and state-preparing the atoms for the experiments of a Raman atomic interferometer.

References

[1] Kasevich M A, Riis E, Chu S and de Voe R G 1989 *Phys. Rev. Lett.* **63** 612

[2] Oates C W, Vogel K R and Hall J L 1996 *Phys. Rev. Lett.* **76** 2866

[3] Adams C S, Sigel and Mlynek J 1994 *Phys. Rep.* **240** 143

[4] Behringer R E, Natarajan V and Timp G 1996 *Appl. Phys. Lett.* **68** 1034

[5] Anderson M H, Ensher J R, Matthews M R, Wieman C E and Cornell E A 1995 *Science* **269** 198

[6] Buell W F 1998 *Laser Part. Beams* **16** 627

[7] Lee H S, Park S E, Kwon T Y, Yang S H and Cho H 2001 *IEEE Trans. Instrum. Meas.* **50** 531

[8] Slowe C, Vernac L and Hau L V 2005 *Rev. Sci. Instrum.* **76** 103101

[9] Bell S C, Junker M, Jasperse M, Turner L D, Lin Y J, Spielman I B and Scholten R E 2010 *Rev. Sci. Instrum.* **81** 013105

[10] Balykin V I, Letokhov V S and Mushin V I 1979 *JETP Lett.* **29** 560

[11] Riis E, Weiss D S, Moler K A and Chu S 1990 *Phys. Rev. Lett.* **64** 1658

[12] Dieckmann K, Spreeuw R J C, Weidemüller M and Walraven J T M 1998 *Phys. Rev.* A **58** 3891

[13] Kim K H, Lee K I and Noh H R 2001 *Phys. Rev.* A **64** 013402

[14] Kohel J M, Ramirez-Serrano J and Thompson R J 2003 *J. Opt. Soc. Am.* B **20** 1161

[15] Schoser J, Batär A and Löw R 2002 *Phys. Rev.* A **66** 023410

[16] Lu Z T, Corwin K L and Renn M J 1996 *Phys. Rev. Lett.* **77** 3331

[17] Feng Y Y, Zhu C X, Wang X J, Xue H B, Ye X Y and Zhou Z Y 2009 *Chin. Phys.* B **18** 3373

[18] Metcalf H J and van der Straten P 1999 *Laser Cooling and Trapping* (New York: Springer-Verlag) p. 32

[19] Monroe C, Swann W, Robinson H and Wieman C 1990 *Phys. Rev. Lett.* **65** 1571